AVIAN DISEASES 54:981–989, 2010

Forensic Investigation of a 1986 Outbreak of Osteopetrosis in Commercial Brown Layers Reveals a Novel Avian Leukosis Virus–Related Genome

Taylor Barbosa,[A] Marcia Ramirez,[B] Scott Hafner,[C] Sunny Cheng,[A] and Guillermo Zavala[AD]

[A]Poultry Diagnostic and Research Center, Department of Population Health, University of Georgia, 953 College Station Road, Athens, GA 30602
[B]Laboratorio de Patología Aviar, Escuela de Medicina Veterinaria, Universidad Nacional de Costa Rica, Apartado 86-3000, Heredia, Costa Rica
[C]Pathology Section, USDA FSIS, Eastern Laboratory, Russell Research Center, P.O. Box 6085, College Station Road, Athens, GA 30604

Received 15 November 2009; Accepted and published ahead of print 14 March 2010

SUMMARY. Avian leukosis virus (ALV) is known to cause several neoplastic conditions in chickens, such as B-cell lymphomas, myelocytomas, erythroblastosis, and other types of neoplasia including osteopetrosis. We describe herein the identification of unique ALV-related proviral DNA sequences in an archived chicken bone affected with osteopetrosis. The osteopetrotic bone was obtained from an affected 46-week-old brown layer during an outbreak of osteopetrosis in Costa Rica in 1986. Analysis of proviral DNA in the 23-year-old osteopetrotic bone revealed unique exogenous ALV-related sequences that were named CR-1986 (Costa Rica, 1986). The 5′ and 3′ long terminal repeats (LTR) in the proviral DNA were identical to each other. The U3 regions in the LTRs were most similar to equivalent sequences in ALV-J, while U5 was identical to known endogenous ALV-E sequences. The predicted CR-1986 envelope protein was most similar to the envelope of myeloblastosis associated virus type 1 (MAV-1), although the percentage of amino acid sequence similarity to MAV-1 was low (90.4%). The variable and hypervariable regions of gp85 displayed several mutations compared to representative strains of ALV. The gp37 (transmembrane or TM) envelope protein showed three leucine to serine mutations that may represent important changes in the conformation of this protein, a finding that is currently being investigated. Several recombination events may have contributed to the emergence of CR-1986 because each analyzed segment was similar to a different ALV. CR-1986 may represent a unique ALV based on distinctive characteristics of its predicted envelope protein in comparison to previously reported ALVs.

RESUMEN. Investigación forense de un brote de osteopetrosis en ponedoras comerciales marrones en el año 1986 revela un nuevo genoma relacionado con el virus de la leucosis aviar.

Se sabe que el virus de la leucosis aviar (ALV) causa varias enfermedades neoplásicas en los pollos, como los linfomas de células B, mielocitomas, eritroblastosis, y otros tipos de neoplasias como la osteopetrosis. En este trabajo se describe la identificación de secuencias de ADN provirales únicas relacionadas con el virus de la leucosis aviar en un hueso archivado perteneciente a un pollo afectado con osteopetrosis. El hueso con osteopetrosis se obtuvo de una gallina de postura marrón de 46 semanas de edad, afectada durante un brote de osteopetrosis en Costa Rica en el año 1986. El análisis del ADN proviral en el hueso con osteopetrosis de 23 años de edad, reveló la presencia de secuencias relacionadas con un virus exógeno único de la leucosis aviar que fue nombrado CR-1986 (Costa Rica, 1986). Las secuencias terminales repetidas largas (con las siglas en inglés LTR) de los extremos 5′ y 3′ del ADN proviral eran idénticas entre sí. Las regiones U3 en las secuencias terminales largas eran más similares a las secuencias equivalentes del virus de la leucosis aviar J (ALV-J), mientras que la región U5 era idéntica a las secuencias conocidas de los virus endógenos de la leucosis aviar E. La secuencia predicha de la proteína de la envoltura del virus CR-1986 era más similar a la envoltura del virus tipo 1 asociado a la mieloblastosis (MAV-1), aunque el porcentaje de similitud con la secuencia de aminoácidos del MAV-1 fue baja (90.4%). Las regiones variables e hipervariables de gp85 mostraron varias mutaciones en comparación con las cepas representativas del virus de la leucosis aviar. La proteína gp37 (transmembrana o TM) de la envoltura, muestra tres mutaciones de leucina a serina que pueden representar importantes cambios en la conformación de esta proteína, este es un hallazgo que actualmente está siendo investigado. Varios eventos de recombinación pudieron haber contribuido a la aparición de CR-1986, ya que cada segmento analizado mostró similitud con un virus de la leucosis aviar diferente. El virus CR-1986 puede representar un virus de la leucosis aviar único con base en las características distintivas de la proteína predicha de la envoltura en comparación con los virus de la leucosis reportados anteriormente.

Key words: osteopetrosis, avian leukosis virus, myeloblastosis-associated virus

Abbreviations: ALSV = avian leukosis-sarcoma virus; ALV = avian leukosis virus; IFP = internal fusion peptide; LTR = long terminal repeat; MAV = myeloblastosis-associated virus; PPT = polypurine tract; R = repeat; SU = surface; TM = transmembrane

The avian leukosis-sarcoma viruses (ALSVs) of chickens are classified into six groups (A, B, C, D, E, and J) based on their host range, cross-neutralization, and viral interference. Closely related viruses such as avian myeloblastosis virus and myeloblastosis-associated virus (MAV) have also been reported. ALSVs induce a variety of neoplasms in chickens, such as B-cell lymphomas, myelocytomas, erythroblastosis, and other types of neoplasia, including osteopetrosis.

Avian osteopetrosis is a neoplastic condition in which the long bones of the limbs become abnormally enlarged because of periosteal hyperplasia, which can lead in advanced cases to a characteristic ''boot-like'' appearance of the shanks (16). Although the bones of the limbs are preferentially affected, other bones can also be involved. The lesions are usually bilateral and symmetrical. As lesions progress the proliferation extends towards the metaphysis with ensuing accumulation of spongy, thickened periosteal tissue, which gives the bones a fusiform appearance (17). A severe enlargement of the periosteum can eventually lead to obliteration of the bone marrow cavity, resulting in crippled, anemic, and immunosuppressed chickens (16). Lymphoid leukosis may also

[D]Corresponding author. E-mail: gzavala@uga.edu

occur in some birds affected with osteopetrosis (14). Osteopetrotic chicks may exhibit a stunting syndrome as their growth is significantly delayed (2). The relative mass of the lymphoid organs can be reduced, whereas the mass of the heart, pancreas, kidneys, lungs, brain, liver and bones of osteopetrotic chicks may increase due to edema (2).

Avian leukosis virus (ALV)-induced osteopetrosis results from viral infections causing abnormal growth and differentiation of osteoblasts (21). Initially the osseous collagen content may remain normal and early lesions of osteopetrotic bones may be associated with hypomineralization, but later they become more fully mineralized (2). Viruses that cause osteopetrosis undergo an atypical life cycle involving the persistent synthesis of viral DNA in osteoblasts (20). This atypical life cycle results in osteopetrotic bones containing an average of 5 to 10 copies of integrated and nonintegrated proviral DNA per cell (20). After the onset of lesions, unintegrated viral DNA appears in the transformed osteoblasts (1). Osteopetrotic lesions have been shown to be nonclonally derived, making them different from most other ALV-induced tumors (1). It is still unclear exactly which genetic sequences of ALV are responsible for the development of osteopetrosis but the envelope gene, the long terminal repeat (LTR), and the 5′ end noncoding region (5,19,22) have all been implicated in the ability of some ALV isolates to induce osteopetrosis.

MATERIAL AND METHODS

Case history. During 1986 an adult commercial brown layer flock housed in Costa Rica experienced an outbreak of osteopetrosis. The affected flock was 46 weeks of age at the time of clinical examination and diagnosis. The flock size was approximately 4500 layers in total, and approximately 40% of the hens were clinically affected. Clinical signs included reluctance to move, decreased feed consumption, and decreased egg production, but mortality was not deemed significant. A turkey herpes virus–based Marek's disease vaccine was the sole vaccine administered at the source hatchery. Live birds were sent to Dr. Marcia Ramirez at the Avian Pathology Laboratory, National University of Costa Rica, Heredia, Costa Rica. A diagnosis of osteopetrosis was made based on clinical and *post mortem* observations at the farm and gross and microscopic lesions in birds submitted to the laboratory. Selected bones from affected chickens were cleaned, desiccated, and kept in a glass container at room temperature for 23 years. One specimen from the bone collection was selected for the present study.

DNA extraction. The DNA extraction procedure used was a modification of a protocol previously described by Ye *et al.* (26). A 3-mm transverse section of the specimen was excised at the level of the diaphysis and the bone tissue was macerated thoroughly to produce a fine powder. The bone material was suspended in 200 µl of digestion buffer (50 mM Tris-HCl, 1 mM EDTA) containing 800 µg/ml of proteinase K and then incubated at 56 C for 2 hr, followed by overnight incubation at 37 C. After digestion was complete, 1 volume of phenol:chloroform (25:24:1) saturated with 10 mM Tris-HCl (pH 8.0) was added, and the mixture was shaken vigorously and then centrifuged at 16,000 × *g* for 10 min. After centrifugation, the supernatant containing DNA was transferred to another tube, the excess phenol was removed with a single wash with chloroform (24:1), and the centrifugation step was repeated. The DNA was precipitated with cold isopropanol and pelleted at 16,000 × *g* for 10 min. The pellet was washed with 75% ethanol and centrifuged at 16,000 × *g* for 5 min. The supernatant was discarded and the precipitate (DNA) was air-dried and then dissolved in 40 µl of sterile double-distilled DNAse- and RNAse-free water.

PCR and real-time PCR. The quality of total genomic bone DNA was tested by TaqMan Real-Time PCR using collagen-specific primers and probe, as described by Islam *et al.* (10). Briefly, iQ Super Kit (BioRad, Hercules, CA) was used per the manufacturer's recommendations. Each reaction contained 0.3 µM of each primer and 0.2 µM of the corresponding probe, 12.5 µl of iQ PCR supermix, and 5 µl of DNA template in a total reaction volume of 25 µl. The cycling parameters were 50 C for 2 min, then 95 C for 2 min followed by 45 cycles consisting of denaturation at 94 C for 10 sec and annealing/extension at 60 C for 45 sec. Amplification and data acquisition were carried out using the thermocycler Chromo4 System for Real-Time PCR Detection (BioRad). PCR amplifications of exogenous and endogenous ALV sequences were attempted using three sets of primers. The first one amplified most of the *env* gene using the BS-up and BS-down primers as described (23). A second fragment was amplified using the Bs-up and the LTR-R (3) primers. The last set of primers was intended to amplify the 5′ end of the proviral DNA, for which the LTR-F and the 7501-AR primers were used (3). All three sets of primers amplify endogenous and exogenous ALV sequences. The PCR amplifications were carried out using a proofreading polymerase enzyme (PlatinumH Pfx DNA polymerase, Invitrogen, Carlsbad, CA) per the manufacturer's recommendations. The PCR products were visualized in an agarose gel using a Dark Reader (Clare Chemical Research, Dolores, CO), which does not use ultraviolet light, which could cause cDNA damage. Specific products (1.5 kb for the BS-up:BS-down primers; 2.5 kb for the BS-up:LTR-R; and 600 bp for the LTR-F:7501-AR) were gel-purified using a commercial gel extraction kit (QIAquick Gel Extraction Kit, Qiagen, Valencia, CA). The purified products were cloned separately into pCR2.1 plasmids following the manufacturer's recommendations (Topo cloning kit, Invitrogen). After screening and purification, the plasmids were used as templates for sequencing using the dideoxynucleotide method with the BigDye v3.1 terminator kit (Applied Biosystems, Foster City, CA). Sequencing readings were performed in an ABI PRISM^{TM} 377 sequencer (Perkin Elmer Corp., Waltham, MA). Sequencing primers included the plasmids M13F and M13R (Topo cloning kit) and ALV primers Env-540F 5′-TAG GTT CCC AGT CTC TCC-3′, Env-1162F 5′-AGG CAA ACT TAC CAT GTT AG-3′, Env-1340R 5′-GCC TGT TTA ACG GAC CAA C-3′, and polypurine tract (PPT)-F 5′-AGC AGT ACA TGG GTG GTG G-3′.

Sequence analyses. The overlapping fragments from the cloned sequences were aligned for preparation of contiguous sequences using the Seqman 8 function in the Lasergene 8.0 sequence analysis software (DNASTAR, Inc., Madison, WI). The sequences resolved were aligned with sequences available in GenBank using the ClustalW alignment with weighted residues method in the MegAlign 8.0 sequence analysis function in Lasergene (DNASTAR). The predicted protein phylogenetic tree was constructed with predicted gp85 full-length proteins of ALV representative strains. Protein sequences were compared for similarity using ClustalW and branching was done using the neighbor-joining method with 1000 bootstrap replicates (MegAlign 8.0). ALV representative strains were used for alignments in the sequence analyses and included ALV-A [RCASBP(A)] (9); ALV-B [RCASBP(B)] (9); ALV-C (GenBank AF033808, RSV-C); ALV-RAV-7 (GenBank M16580); ALV-D (GenBank D10652, RSV-D); *ev*-1 (endogenous virus 1; GenBank AY013303); ALV-J (GenBank AY027920, ADOL 7501); MAV-ACMHBIPB (GenBank M11784); RAV-2 (ALV-B) (GenBank K02374, RAV-2); MAV-1 (GenBank L10922); MAV-2 (GenBank L10924); MAV-1/2 (GenBank L10923); MAV Isolate 1 (GenBank AF507028); MAV Isolate 18 (GenBank AF507030); MAV Isolate 25 (GenBank AF507032); RSV-A (GenBank M14901); PDRC-3246 (ALV-A/E) GenBank EU700901; ALV-E (GenBank AY013305); RAV-2 (GenBank M14902); RSV-B (GenBank AF052428); MAV Isolate 26 (GenBank AF507033); ALV-F (GenBank AY608692); ALV-J (UD5, GenBank AF307952); ALV-J (SD07LK2, GenBank EU264065).

Histopathology. A 4-mm cross-section of the bone specimen (metatarsus) was excised at the level of the diaphysis and used for microscopic examination. Such transverse section was demineralized using standard bone histology procedures. Briefly, a segment of the bone was removed and placed in a concentrated acid solution; the solution was continuously stirred until gross examination of the bone revealed that decalcification had occurred.

Table 1. Amino acid percentage similarity and nucleotide percentage identity between CR-1986 and reference ALV strains.

Virus subgroup[A]	Region									
	env[B]	gp85[B]	gp37[B]	PPT[C]	LTR[C]	U3[C]	R[C]	U5[C]	R-Ψ[C]	Ψ[C]
RCASBP-A	88.2	89.2	86.7	45.7	82.1	80.8	82.6	88.2	83.8	74.2
RCASBP-B	82.4	80.5	86.2	45.7	82.1	80.8	82.6	88.2	83.8	74.2
ALV-RAV7	NA[D]	NA	NA	**93.4**[E]	NA	NA	NA	NA	NA	NA
ALV-C	87.5	86.4	**89.3**	59.1	81.1	82.2	87.0	93.4	91.4	89.0
RSV-D	85.5	84.6	87.2	ND[F]	**84.9**	82.6	82.6	93.4	84.8	74.2
ev-1	86.3	85.1	89.2	53.7	53.3	28.0	91.3	**100.0**	91.3	83.3
ALV-J	48.4	42.0	55.6	58.8	84.6	**85.0**	**100.0**	86.8	89.9	87.4
MAV- ACMHBIPB	NA	NA	NA	NA	80.8	78.9	82.6	88.2	91.0	88.7
RAV-2	NA	NA	89.7	85.9	80.4	78.9	82.6	86.8	**91.7**	**90.8**
MAV-1	**90.4**	**91.0**	**89.3**	61.7	45.2	28.6	91.3	89.5	86.3	76.8
MAV-2	90.1	82.8	**89.3**	61.3	45.5	31.9	91.3	86.8	85.8	76.8
MAV-1/2	85	90.5	**89.3**	61.7	45.5	31.9	91.3	86.8	85.8	76.8

[A]ALV-A [RCASBP(A)]; ALV-B [RCASBP(B)]; ALV-RAV7 (GenBank M16580);ALV-C (GenBank AF033808, RSV-C); ALV-D (GenBank D10652, RSV-D); *ev*-1 (GenBank AY013303); ALV-J (GenBank AY027920, Adol 7501); MAV ACMHBIPB (GenBank M11784); RAV-2 (ALV-B, GenBank K02374); MAV-1 (GenBank L10922); MAV-2 (GenBank L10923); MAV-1/2 (GenBank L10924).
[B]Amino acid.
[C]Nucleotide.
[D]NA = sequences not available for comparison.
[E]Bolded values represent the highest amino acid similarities found.
[F]ND = not done.

Once demineralized, the cross-section of bone was processed using standard histology procedures and embedded in histology-grade paraffin to prepare thin (4–6 μm) tissue sections that were stained with hematoxylin and eosin prior to examination with light microscopy. Because it was necessary to demineralize the bone tissue, bone density was expected to be diminished compared to the original desiccated bone specimen.

RESULTS

Genomic DNA was successfully isolated and purified from the archived bone specimen even though no special care had been taken to preserve the proviral DNA and the bone had been at room temperature in a glass jar and exposed to natural environmental conditions for 23 years. The real-time PCR targeting the collagen gene was positive in all DNA isolation attempts (results not shown). Based on the description of the clinical signs and lesions, and the gross appearance of the affected bones we hypothesized that the cause of the outbreak was a retrovirus belonging to the avian leukosis-sarcoma group of retroviruses (ALSVs). Aiming to identify any ALSV group–related virus sequences, ALV-specific PCR primers were used targeting the 5′ end and 3′ end of the predicted integrated ALV proviral DNA. The LTR-F:7501-AR primer pair was used to amplify a product of approximately 600 bp, located in the 5′ end of proviral DNA. We also used two different primer sets targeting the envelope region. The BS-up:BS-dwn primer set rendered a 1.5-kb fragment and the Bs-up:LTR-R primer set amplified a 2.5-kb fragment. As described, all three fragments were cloned separately in the sequencing vector pcR2.1. Plasmids positive for the respective inserts were selected and used for direct sequencing.

All selected plasmid inserts were successfully and fully sequenced. For each PCR product, five clones were selected and sequenced individually. Two out of five of the LTR-F:7501-AR fragments, three out of five of the BS-up:BS-dwn fragments, and three out of five Bs-up:LTR-R fragments were identified as endogenous ALV sequences (results not shown) and were discarded from further analysis. All of the nonendogenous nucleotide sequences were 100% identical to each other for each respective fragment. In addition, the BS-up:BS-dwn and the Bs-up:LTR-R overlapping fragments shared sequences that were 100% identical for regions where such fragments overlapped. For the analysis of the proviral DNAs, we constructed two different contiguous sequences (contigs), one containing the 5′ end (the entire 5′LTR to the first 38 nucleotides in the 5′ end of the *gag* gene); and another one for the *env*-3′LTR region. Both contigs were blasted using the NCBI blastn tool. Full fragment blasting did not identify any sequences available in public databases with high similarity (above 95%) to our sequences. However, all of the first 100 hits corresponded to viruses belonging to the ALSV group. These results provided clear evidence that ALSV-related proviral DNA sequences were present in the osteopetrotic bone, but such sequences were not highly similar to proviral sequences from previously studied or published ALSVs. We named the newly identified sequence CR-1986 (Costa Rica, 1986). The CR-1986 sequence is deposited in GenBank under the accession number GU002400. For further analysis of the contigs the CR-1986 sequences were aligned with ALSV reference viruses (at least one from each recognized exogenous virus subgroup). Table 1 shows a summary of the results of such alignments.

Analysis of the complete *env* gene amino acid sequence in the CR-1986 provirus revealed that the most similar corresponding proviral sequence was that of MAV-1. However, the amino acid sequence similarity between these two viruses was only 90.4%. When analyzed separately, the predicted amino acid sequences of the surface (SU or gp85) and transmembrane (TM or gp37) regions of the of the viral envelope were 91.0% similar between MAV-1 and CR-1986 for gp85; and a similarity of 89.3% was identified between CR-1986, MAV-1, MAV-2, and ALV-C for gp37. The gp85 region of the viral envelope is the most important in determining the subgroup of ALSV. Figs. 1 and 2 show the gp85 and gp37 sequence alignments for CR-1986 and ALV representative strains, respectively.

The 3′ noncoding region of the proviral DNA was also analyzed in the present study. The CR-1986 PPT region was not identical to any of the representative strains herein examined. Blasting of the CR-1986 PPT region sequence showed an identity of 93.4% between CR-1986 and RAV-7, an ALV classified as ALV-C (15).

Analysis of the 5′ and 3′ proviral CR-1986 LTRs showed relevant characteristics. Both LTRs were identical, indicating that despite amplification and sequencing of two separate fragments in the

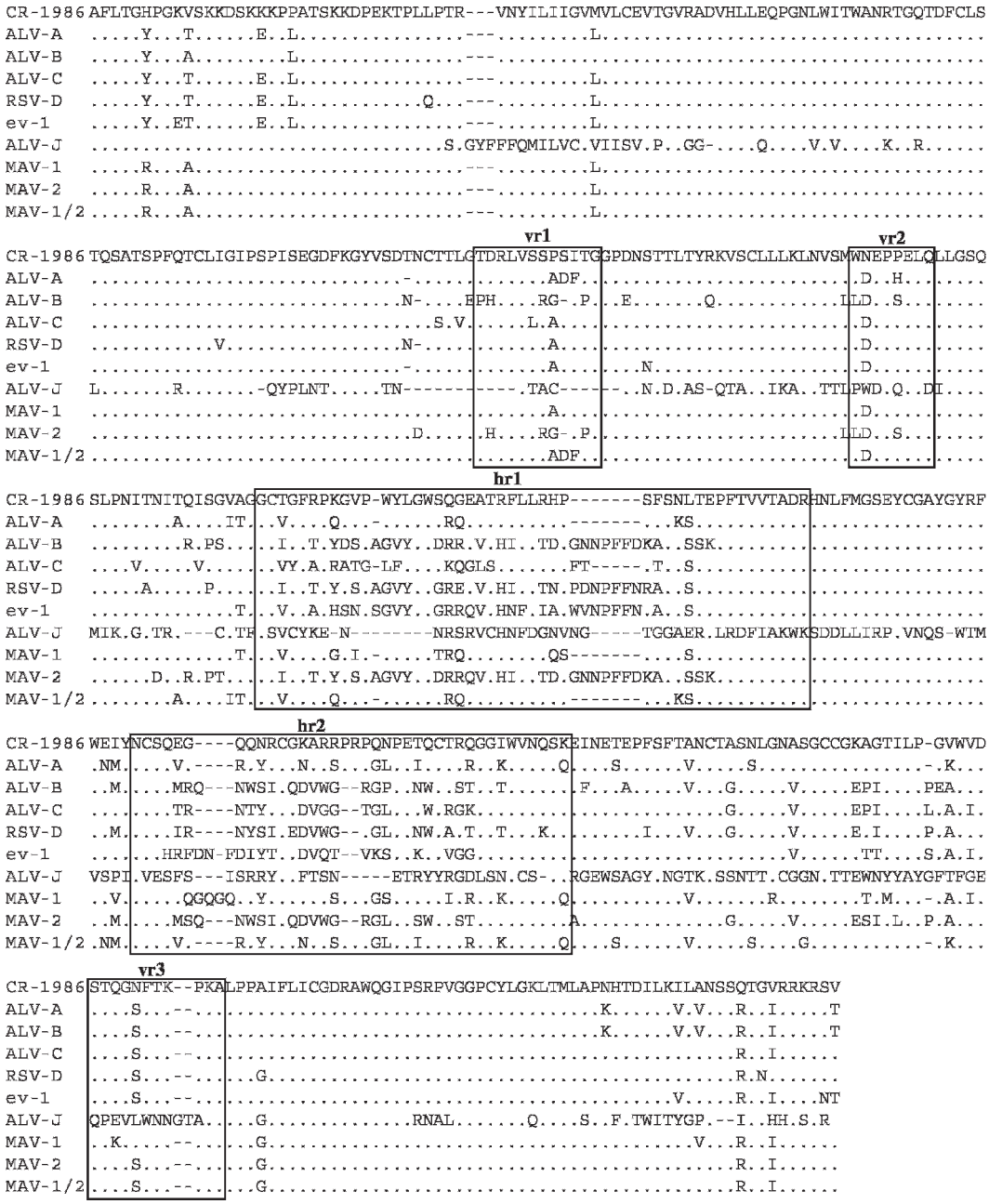

Fig. 1. Alignment of deduced amino acid sequences of gp85 (surface envelope protein or SU) of the CR-1986 (GenBank GU002400) and representative ALVs. ALV-A [RCASBP(A)]; ALV-B [RCASBP(B)]; ALV-C (GenBank AF033808, RSV-C); RSV-D (GenBank D10652, ALV-D); ALV-J (GenBank AY027920, ADOL 7501); *ev*-1 (GenBank AY013303); MAV-1 (GenBank L10922); MAV-2 (GenBank L10924); MAV-1/2 (GenBank L10923). Boxes represent the variable (vr) and hypervariable (hr) regions. Positions of identity are indicated by dots, whereas nucleotide differences are appropriately marked. Dashes (−) represent gaps produced in the alignment.

proviral genome, both belong to a common source. As a whole, the CR-1986 LTR is 312 bp long and displayed the highest identity to ALV-D (84.9%). However the U3 region (Fig. 3), which is probably most important for viral replication and transcription (27), exhibited an identity of 85% to the ALV-J representative virus. The repeat (R) region was identical to ALV-J and the U5 region was identical to *ev*-1.

A comparative analysis of the 5′ end of the genomic DNA is shown in Fig. 4. This sequence was 91.7% similar to RAV-2 (ALV-B). The 5′ leader sequence (noncoding region located just upstream from the *gag* gene) shows an insertion of a 19 bp direct repeat 17 nucleotides upstream from the *gag* starting codon. The splice donor site is conserved in all analyzed sequences.

Fig. 5 shows the osteopetrosis lesions in a 46-week-old brown leghorn egg layer affected in the outbreak herein reported. As seen in Fig. 5, the bone marrow space was almost completely obliterated. Histopathology examination revealed a nearly completely obliterated medullary cavity of the decalcified cross-section with proliferation of compactly arranged, interconnected bone trabeculae. Such trabeculae were separated by irregularly shaped and variably sized spaces (dilated haversian and Volkmann's canals) which, in some areas, were radially arrayed. The most dilated canals tended to be

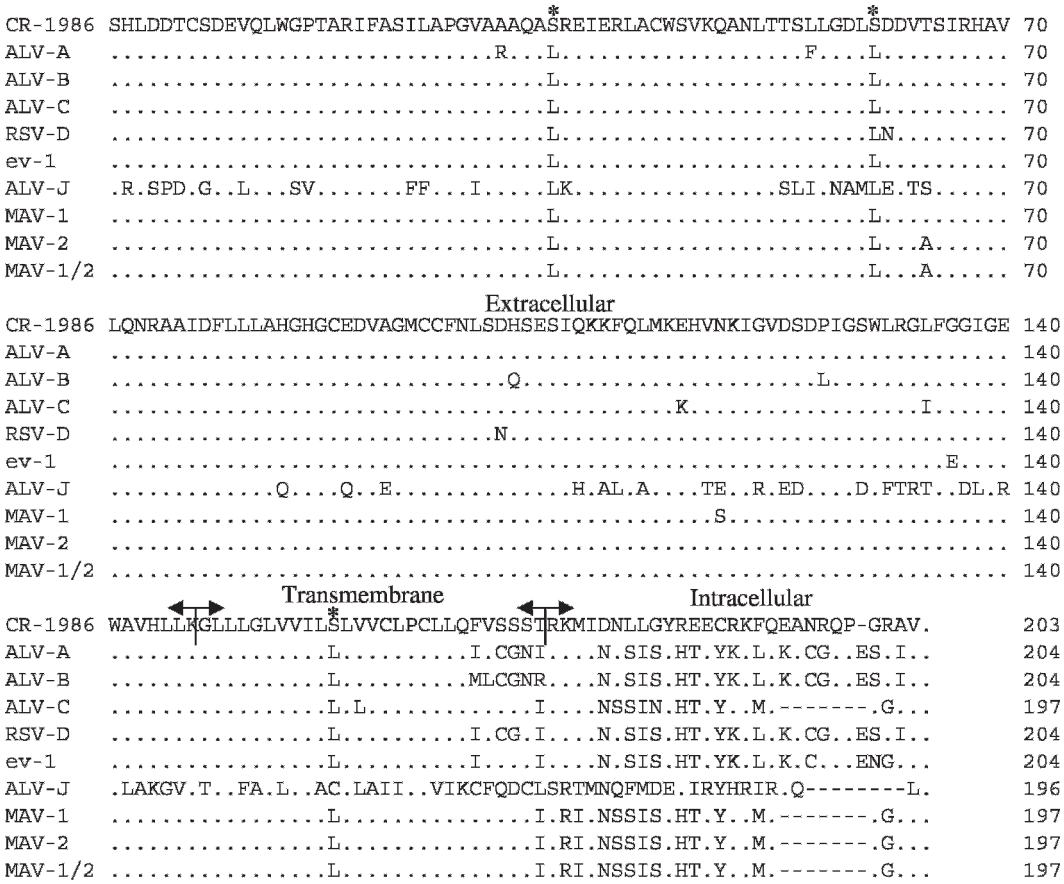

Fig. 2. Alignment of deduced amino acid sequences of gp37 (transmembrane env protein) of the CR-1986 (GenBank GU00240) and representative ALVs. ALV-A [RCASBP(A)]; ALV-B [RCASBP(B)]; ALV-C (GenBank AF033808, RSV-C); ALV-D (GenBank D10652, RSV-D); ALV-J (GenBank AY027920, ADOL 7501); *ev*-1 (GenBank AY013303); MAV-1 (GenBank L10922); MAV-2 (GenBank L10924); MAV-1/2 (GenBank L10923). Positions of identity are indicated by dots, whereas nucleotide differences are appropriately marked. Dashes (−) represent gaps produced in the alignment. Leucine to serine point mutations are annotated with an asterisk (*). Major domains are indicated.

peripherally located and some canals extended through the outer layer. Haversian systems are often irregularly shaped with a marked variation in size and osteocytic lacunae appear numerous and are moderately enlarged. The bone matrix ranged from intensely eosinophilic to basophilic with the basophilic matrix being most prominent in the interstitial systems interposed between Haversian systems.

DISCUSSION

The gp85 region of the viral envelope is most important in determining the subgroup of ALSV based on virus–host interactions (18). The gp85-predicted amino acid sequence alignment is shown in Fig. 1, in which the variable and hypervariable regions are indicated. The variable regions of the CR-1986 provirus are most similar to ALV-A, MAV-1, and MAV-1/2, but such variable regions displayed several mutations. The hypervariable regions exhibited much higher variation, with the MAV-1 and ALV-A sequences being most similar to the CR-1986 sequence. The percent similarities between various regions of the CR-1986 genome and of selected members of the ALSV group are indicated in Table 1. Previous work suggested that MAV-1/2 and MAV-2 can be closely associated with osteopetrosis in chickens, and that their envelope genes display significant differences in the SU protein compared to MAV-1, which is rather prone to inducing nephroblastomas (11). However, the CR-1986 SU protein sequences are more closely related to MAV-1 and ALV-A, neither one of which is commonly associated with osteopetrosis. It is possible that a combination of mutations present in the CR-1986 genome might have led to the development of osteopetrotic bones, despite differences from MAV-2. Specific mutations in the transmembrane protein (gp37) observed in MAV-2 have been correlated to osteopetrosis (11). Specifically, the replacement of a threonine by an alanine residue in the MAV-2 compared to MAV-1 (in amino acid position 64 of gp37, Fig. 2) has been suspected of causing a higher incidence of osteopetrosis in MAV-infected chickens (11). The CR-1986 TM protein sequence does not contain such alanine residue present in the MAV-2 sequence and it contains instead a threonine residue as most of the other ALVs analyzed (Fig. 2). The absence of this mutation in the CR-1986 *env* sequence suggests that possibly one or more other mutations were responsible for this virus causing osteopetrosis. It remains to be determined whether CR-1986 was indeed responsible for the development of osteopetrosis in the present case. Further analysis of the gp37 sequence revealed three point mutations, where a nonpolar neutral strongly hydrophobic leucine (L) was replaced by a polar neutral serine (S). These mutations are localized on the extracellular domain and inside the transmembrane domains of gp37, which could potentially induce a significant change in the secondary structure of its extracellular domain. Further studies are

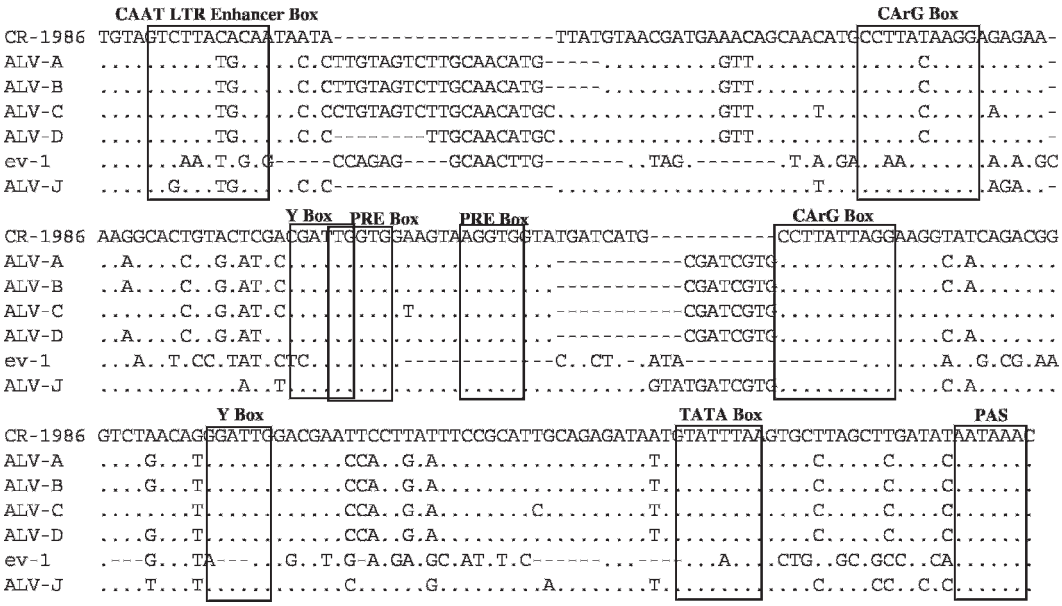

Fig. 3. DNA sequence comparison of the ALV U3 region within LTR of the CR-1986 (GenBank GU002400) and representative ALVs. ALV-A [RCASBP(A)]; ALV-B [RCASBP(B)]; ALV-C (GenBank AF033808, RSV-C); ALV-D (GenBank D10652, RSV-D); *ev*-1 (GenBank AY013303); ALV-J (GenBank AY027920, ADOL 7501). Positions of identity are indicated by dots while nucleotide differences are appropriately marked. Dashes (−) represent gaps produced in the alignment. Location of putative transcription regulatory elements are indicated in boxes and labeled. PAS = polyadenylation signal.

necessary to investigate the significance of these mutations on the ability of CR-1986 causing osteopetrosis. Of particular interest are two mutations, one located in the transmembrane domain of gp37 (L158S), and the second located in the membrane fusion peptide (L35S) (6). The fusion peptide of ALSV known as internal fusion peptide (IFP) is a region within the TM protein that is crucial for binding and destabilizing target membranes (8). It has been proposed that the envelope protein undergoes conformational changes triggered by its binding to the receptor on the target cell surface (e.g., Tva for ALV-A), exposing the hydrophobic IFP domain to destabilize the cell membrane prior to membrane fusion similar to the function of influenza virus hemagglutinin and HIV-1 gp41 (7). As the Leu23 of this IFP is highly conserved among members of ALSV (amino acid position 35 of gp37, Fig. 2), it would be interesting to study the effects of the serine substitution on membrane fusion and the ability of ALSV to infect different types of cells.

PPT is an important region of the retrovirus genome that plays a relevant role during reverse transcription. The CR-1986 PPT region was not identical to any of the ALV representative strains. An ALV-C isolate (RAV-7) (15) revealed the highest nucleotide identity to CR-1986 in this region (93.4%). However, the published sequences of RAV-7 only included a short sequence spanning the 3′ end, not allowing for any further comparisons besides the PPT region.

A comparison of the known regulatory and transcriptional elements in the U3 of ALSV is highlighted in Fig. 3. Based on this analysis, it is clear that the CR-1986 sequences are of exogenous origin, since all of the known regulatory elements are very similar to exogenous ALVs. Presence of these regulatory sequences within U3 suggests the potential ability of CR-1986 to replicate in high levels and cause disease (27). MAV-related LTR sequences were not included in the alignment since they have a much longer region resulting from several insertions compared to other exogenous ALVs (11). The analysis also suggested that the origin of the CR-1986 LTR is related to an exogenous ALV, albeit not from an MAV-related virus, in contrast with the finding that suggested higher similarity to MAV-related viruses in the *env* gene sequences. The composition of CR-1986 LTR likely being part exogenous (U3 and R) and part endogenous (U5), raises the question of the possible origin of CR-1986. It is unlikely that this combination alone would enable CR-1986 to cause osteopetrosis (16).

Recombinant viruses between RAV-0 (ALV-E) and the isolate Br21 indicated that 5′ sequences that affected osteopetrotic potential resided in an 834-bp region near the 5′ LTR (19). Although a number of mutations were seen on the 5′ end noncoding region of CR-1986 compared to other ALV sequences (Fig. 4), at this point their significance is not known. It has been postulated that similar mutations in the same region may alter packaging of genomic RNA leading to accumulation of extra copies of unintegrated viral DNA inside the infected cell, one of the factors directly related to osteopetrosis (21). Also, CR-1986 shows a 17-bp insertion before the *gag* starting codon. Two other viruses with similar insertions have been published in GenBank and they are included in Fig. 4 [RAV-2 (ALV-B) (GenBank K02374) and a MAV-related virus (GenBank M11784)]. Such repeat insertions are not likely to be specific to any particular subgroup of ALV. The significance of this sequence remains obscure and it may represent only a random mistake generated during reverse transcription.

Retroviruses are well known for their high variability and high mutation rates (24,25). Natural recombination of ALVs has been reported, possibly facilitating the emergence of novel subgroups (3,4,12,13). We describe herein partial sequences of a unique ALV-related genome that was isolated from an osteopetrotic bone that had been archived for 23 years. It is clear that the CR-1986 proviral DNA is different from all other reported ALV sequences to date. We speculate that CR-1986 originated by normal mutation and/or by recombination of various ALVs, since each analyzed segment was similar to a different ALV representative. Because the proviral sequence of the CR-1986 *env* gene appeared to be significantly different from *env* sequences belonging to other known ALV

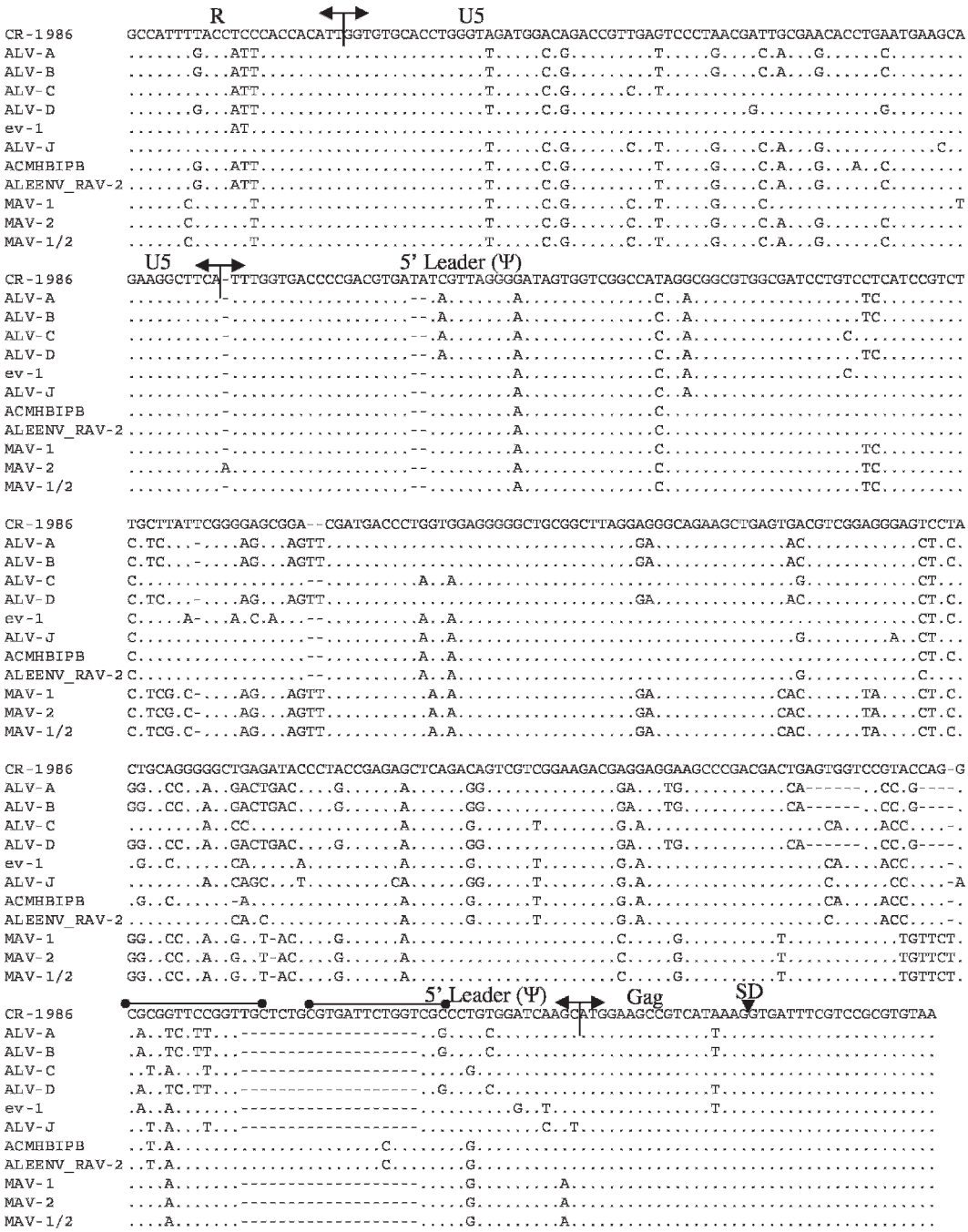

Fig. 4. DNA sequence comparison of the ALV 5′ end region of the CR-1986 (GenBank GU002400) and representative ALVs. ALV-A [RCASBP(A)]; ALV-B [RCASBP(B)]; ALV-C (GenBank AF033808, RSV-C); ALV-D (GenBank D10652, RSV-D); *ev*-1 (GenBank AY013303); ALV-J (GenBank AY027920, ADOL 7501); ACMHBIPB MAV (GenBank M11784); ALEENV_RAV-2 (ALV-B, GenBank K02374); MAV-1 (GenBank L10922); MAV-2 (GenBank L10924); MAV-1/2 (GenBank L10923). Positions of identity are indicated by dots, whereas nucleotide differences are appropriately marked. Dashes (−) represent gaps produced in the alignment. Genomic regions are indicated on top of the alignment. Repeat sequences are indicated with a bold line flanked by closed circles. R = Repeat; U5 = unique 5′ end; 5′ Leader Ψ = part of the encapsidation signal, 5′ end noncoding region; SD = splice donor.

subgroups (Fig. 6), we suggest that CR-1986 may represent a novel ALV subgroup or at least an unusual ALV-related virus. The phylogenetic analysis of the entire gp85 protein is presented in Fig. 6. Clearly, CR-1986 does not group with any previously reported ALV subgroup, an observation supported by high bootstrap values in the alignments. The alignments of gp85 (Fig. 1) suggested that CR-1986 represents a virus partially related to MAV-1 and ALV-A. Since only nucleotide and predicted amino acid sequences could be studied and because a replicating CR-1986 virus is not available we could not study virus–host interactions. Reverse genetics studies are being conducted in our laboratory to develop an infectious clone bearing some of the genes and sequences identified in CR-1986. These studies should allow for evaluation of replication and pathogenesis of CR-1986 as well as virus–host interactions that should reveal whether CR-1986 belongs to any of the known ALV subgroups.

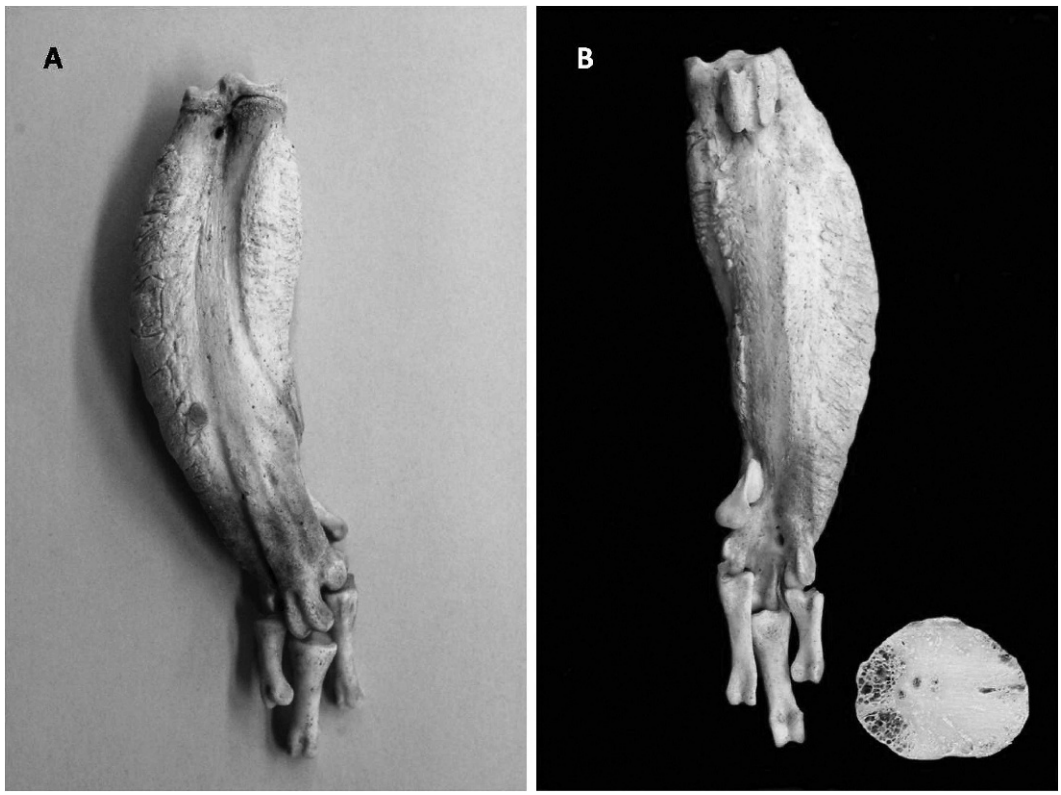

Fig. 5. Osteopetrosis lesions from a 46-week-old brown leghorn egg layer affected during a 1986 outbreak of osteopetrosis. (A) Dorsal aspect of an osteopetrotic tarso-metatarsus. (B) Palmar aspect of the bone depicted in A. The insert corresponds to a cross (diaphyseal) section of the bone depicted in both A and B. Note the almost complete obliteration of the bone marrow space.

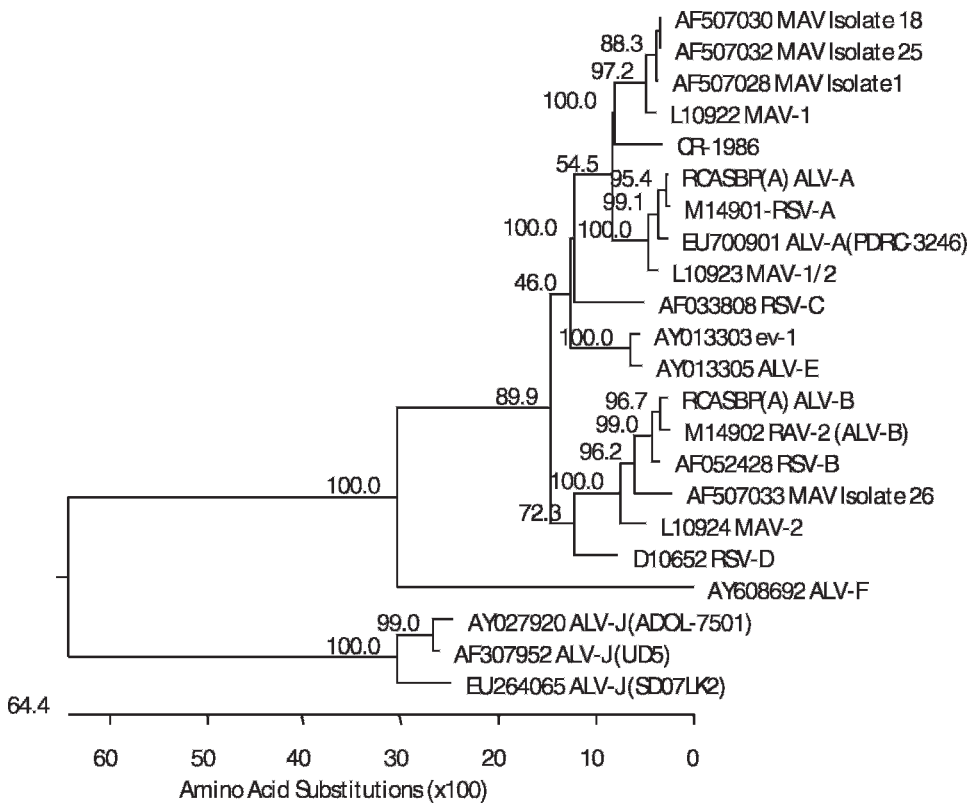

Fig. 6. Phylogenetic tree of full length gp85 (Surface) envelope protein of ALV representative strains. Tree was constructed using the neighbor-joining method with 1000 bootstrap replicates. Numbers denote the bootstrap confidence interval for 1000 replicates in which a certain branch occurred. Isolate nomenclature represented by GenBank accession number followed by ALV subgroup and name of isolate. The tree is drawn to scale and it represents the number of amino acid substitutions every 100 positions.

REFERENCES

1. Aurigemma, R. E., R. D. Comstock, and R. E. Smith. Persistent viral DNA synthesis associated with an avian osteopetrosis-inducing virus. Virology 171:626–629. 1989.

2. Banes, A. J., and R. E. Smith. Biological characterization of avian osteopetrosis. Infect. Immun. 16:876–884. 1977.

3. Barbosa, T., G. Zavala, and S. Cheng. Molecular characterization of three recombinant isolates of avian leukosis virus obtained from contaminated Marek's disease vaccines. Avian Dis. 52:245–252. 2008.

4. Benson, S. J., B. L. Ruis, A. M. Fadly, and K. F. Conklin. The unique envelope gene of the subgroup J avian leukosis virus derives from ev/J proviruses, a novel family of avian endogenous viruses. J. Virol. 72:10157–10164. 1998.

5. Brown, D. W., B. P. Blais, and H. L. Robinson. Long terminal repeat (LTR) sequences, env, and a region near the 5′ LTR influence the pathogenic potential of recombinants between Rous-associated virus types 0 and 1. J. Virol. 62:3431–3437. 1988.

6. Cheng, S. F., C. W. Wu, E. A. Kantchev, and D. K. Chang. Structure and membrane interaction of the internal fusion peptide of avian sarcoma leukosis virus. Eur. J. Biochem. 271:4725–4736. 2004.

7. Damico, R., and P. Bates. Soluble receptor-induced retroviral infection of receptor-deficient cells. J. Virol. 74:6469–6475. 2000.

8. Gilbert, J. M., L. D. Hernandez, J. W. Balliet, P. Bates, and J. M. White. Receptor-induced conformational changes in the subgroup A avian leukosis and sarcoma virus envelope glycoprotein. J. Virol. 69:7410–7415. 1995.

9. Hughes, S. H., J. J. Greenhouse, C. J. Petropoulos, and P. Sutrave. Adaptor plasmids simplify the insertion of foreign DNA into helper-independent retroviral vectors. J. Virol. 61:3004–3012. 1987.

10. Islam, A., B. Harrison, B. F. Cheetham, T. J. Mahony, P. L. Young, and S. W. Walkden-Brown. Differential amplification and quantitation of Marek's disease viruses using real-time polymerase chain reaction. J. Virol. Methods 119:103–113. 2004.

11. Joliot, V., K. Boroughs, F. Lasserre, J. Crochet, G. Dambrine, R. E. Smith, and B. Perbal. Pathogenic potential of myeloblastosis-associated virus: implication of env proteins for osteopetrosis induction. Virology 195:812–819. 1993.

12. Lupiani, B., H. Hunt, R. Silva, and A. Fadly. Identification and characterization of recombinant subgroup J avian leukosis viruses (ALV) expressing subgroup A ALV envelope. Virology 276:37–43. 2000.

13. Lupiani, B., A. R. Pandiri, J. Mays, H. D. Hunt, and A. M. Fadly. Molecular and biological characterization of a naturally occurring recombinant subgroup B avian leukosis virus with a subgroup J-like long terminal repeat. Avian Dis. 50:572–578. 2006.

14. Mays, J. K., A. R. Pandiri, and A. M. Fadly. Susceptibility of various parental lines of commercial white leghorn layers to infection with a naturally occurring recombinant avian leukosis virus containing subgroup B envelope and subgroup J long terminal repeat. Avian Dis. 50:342–347. 2006.

15. Onuki, Y., A. Ohshima, Y. Kawarabayasi, and T. Takeya. Comparison of the structural organizations in the 3′-terminal regions of five avian retrovirus strains: RAV 7, RAV 50, B77, PR-B, and SR-B. Virology 156:163–166. 1987.

16. Perbal, B. Pathogenic potential of myeloblastosis-associated viruses. Infect. Agents Dis. 4:212–227. 1995.

17. Powers, B. E., R. W. Norrdin, S. P. Snyder, and R. E. Smith. A sequential study of bone lesions caused by isolates of an avian osteopetrosis virus, MAV-2(0). Bone 8:231–240. 1987.

18. Rainey, G. J., A. Natonson, L. F. Maxfield, and J. M. Coffin. Mechanisms of avian retroviral host range extension. J. Virol. 77:6709–6719. 2003.

19. Robinson, H. L., R. G. Foster, B. P. Blais, S. S. Reinsch, M. Newstein, and P. R. Shank. 5′ Avian leukosis virus sequences and osteopetrotic potential. Virology 190:866–871. 1992.

20. Robinson, H. L., and B. D. Miles. Avian leukosis virus-induced osteopetrosis is associated with the persistent synthesis of viral DNA. Virology 141:130–143. 1985.

21. Robinson, H. L., S. S. Reinsch, and P. R. Shank. Sequences near the 5′ long terminal repeat of avian leukosis viruses determine the ability to induce osteopetrosis. J. Virol. 59:45–49. 1986.

22. Shank, P. R., P. J. Schatz, L. M. Jensen, P. N. Tsichlis, J. M. Coffin, and H. L. Robinson. Sequences in the gag-pol-5′env region of avian leukosis viruses confer the ability to induce osteopetrosis. Virology 145:94–104. 1985.

23. Spencer, J. L., B. Benkel, M. Chan, and S. Nadin-Davis. Evidence for virus closely related to avian myeloblastosis-associated virus type 1 in a commercial stock of chickens. Avian Pathol. 32:383–390. 2003.

24. Temin, H. M. Retrovirus variation and evolution. Genome 31:17–22. 1989.

25. Temin, H. M. Retrovirus variation and reverse transcription: abnormal strand transfers result in retrovirus genetic variation. Proc. Natl. Acad. Sci. U. S. A. 90:6900–6903. 1993.

26. Ye, J., A. Ji, E. J. Parra, X. Zheng, C. Jiang, X. Zhao, L. Hu, and Z. Tu. A simple and efficient method for extracting DNA from old and burned bone. J. Forensic Sci. 49:754–759. 2004.

27. Zachow, K. R., and K. F. Conklin. CArG, CCAAT, and CCAAT-like protein binding sites in avian retrovirus long terminal repeat enhancers. J. Virol. 66:1959–1970. 1992.